Hue University Journal of Science: Natural Science
Vol. 131, No. 1B, 59–65, 2022

pISSN 1859-1388
eISSN 2615-9678

Fabrication of TiO_2 nanofibre photoelectrode for photoelectrochemical cells

Nghia Van Nguyen*, Truong Ngoc Khoa Nguyen, Hieu Nhat Hoang

Department of Physics and Materials Science, Faculty of Natural Sciences, Quy Nhon University,
170 An Duong Vuong St., Quy Nhon City, Vietnam

* Correspondence to Nguyen Van Nghia <nguyenvannghia@qnu.edu.vn>

(*Received: 3 August 2021; Accepted: 23 February 2022*)

Abstract. The TiO_2 nanofibres (NFs), prepared with the electrospinning method, acted as the photoanode in a photoelectrochemical cell (PEC) for hydrogen generation. The fabrication parameters of Ti/PVP (polyvinylpyrrolidone) fibres were determined with the field-emission scanning electron microscopy (FE-SEM) method. The structure and morphology of the TiO_2 fibres were characterized by using X-ray diffraction (XRD), FE-SEM, transmission electron microscopy (TEM), and high-resolution transmission electron microscopy (HR-TEM). The average diameter of the TiO_2 fibre is 132 ± 16 nm. A three-electrode potentiostat was used to study the photoelectrochemical properties of the photoanode. The density photocurrent reached the saturation value of 80 $\mu A \cdot cm^{-2}$ at 0.2 V under the irradiation of a Xenon lamp.

Keywords: electrospinning, TiO_2 nanofibres, PEC, photoanode

1 Introduction

Many scientists believe that photochemical water splitting to generate hydrogen is one of the most promising technologies because it is based on converting water with sunlight, an available endless energy source [1]. A photoelectrochemical cell (PEC) is a device integrating light absorption on semiconductor materials and electrochemical processes in the cell. After absorbing the appropriate light photon, oxidation and reduction reactions occur on electrodes to separate water into hydrogen and oxygen [1]. Fujishima and Honda were the first to report the water separation with a PEC by using a titanium dioxide (TiO_2) electrode [1]. In PEC technology, the semiconductor material used as a photoelectrode must satisfy the following two basic conditions. First, the bandgap (E_g) must be greater than 1.23 eV, which is the energy needed for splitting water molecules [1]. Second, for the reaction to occur without applying an external voltage, the conductor band bottom must be higher than the water oxidation level, and the valence band peak must be higher than the hydrogen generation potential. Despite having a large E_g, titanium is still one of the most attractive materials for PEC technology because of its stability to corrosion and photo corrosion, low cost, high availability, and low toxicity [2]. It has the conduction band bottom and valence band top position within the oxidation-reduction potentials of H_2O and thus satisfies the requirements for the water splitting process.

The optical conversion efficiency of the PEC depends primarily on the photoelectrode material. An ideal photoelectrode with high efficiency and stability must satisfy the following requirements: intense light absorption and high electron transportability. Besides the crystal structure, these factors also depend on the structural

morphology of the material. One-dimensional nanostructures, such as nanowires, nanotubes, and nanorods, are the most studied because they can improve carrier transportability. For example, they reduce optical loss thanks to their constant path and anti-reflection resistance [3]. One-dimensional nanostructured TiO_2 is usually fabricated with the electrochemical and hydrothermal methods. For instance, TiO_2 nanotubes with a vertical order on the Ti substrate were manufactured with the electrochemical method [4, 5]. In general, this method is simple and can control the fibre diameter. However, the number of photons absorbed into the material cannot be optimized because of the Ti anode. Other authors, such as Grimes et al. [6] and Qin et al. [7], successfully fabricated TiO_2 with a vertical-ordered nanorod structure on transparent conductive fluorine-doped tin oxide. Its optical current density is rather high, but the rod diameter is relatively large, reducing the surface area.

Besides, electrospinning has also gained researchers' attention because of its simplicity and efficiency in fabricating one-dimensional nanostructure on different materials. This method can control the porosity of the electrode film by controlling the nanofibre size [8]. This technique was invented in the US in 1902, but it was not until the late 20th century that scientists noticed it when making one-dimensional nanomaterials. Using electrospinning, Mali et al. [8] and Li et al. [9] successfully fabricated TiO_2 photoelectrodes with the nanofibre structure.

In this work, the TiO_2 nanofibres fabricated on an indium tin oxide (ITO) substrate by electrospinning act as the photoanode in a PEC.

2 Experimental

2.1 Materials

All chemicals: poly(vinylpyrrolidone) (PVP) ($(C_6H_9NO)_n$, M_w 360000 $g \cdot mol^{-1}$, Sigma-Aldrich Co. Ltd.), ethanol (C_2H_5OH, 99.8%, Duc Giang Co., Vietnam), acetic acid (CH_3CO_2H, 99%, Xilong, China), titanium tetraisopropoxide ($Ti(OiPr)_4$, TTip, 97%, Sigma-Aldrich Co. Ltd.), sodium sulfide (Na_2SO_4, 98%, Sigma-Aldrich Co. Ltd.), and distilled water (18.4 $MW \cdot cm^{-1}$) were used without further purification.

2.2 Preparation of TiO_2 NFs on ITO substrate

Preparation of ITO substrate

Cut the ITO (indium tin oxide, Shenzen, China) sheet into small pieces of about 2 cm^2 (2 × 1 cm). They were cleaned ultrasonically in acetone for 30 min, rinsed with distilled water for 15 min, and dried at 50 °C.

Sample manufacturing process

Dissolve 0.4 g of polyvinylpyrrolidone in 5 mL of ethanol at ambient temperature to obtain an 8% (wt) PVP solution. Then, add 3 mL of acetic acid to the above solution and continue stirring with a magnetic stirrer for 1 h. Finally, add 0.8 mL of titanium (IV) tetraisopropoxide to the solution and stir for 1 h. The resulting solution has a transparent pale-yellow colour.

Suck 3 mL of the above solution into a syringe. The ITO substrate is located at the collector of the electrospinning equipment (Nanobond, Tong Li Co.).

To investigate the surface morphology of Ti/PVP fibres, we conducted the spinning process under the following conditions:

+ Mass ratio of TTip/PVP: 1.5:1, 2:1, 2.5:1, and 3:1.

pISSN 1859-1388
eISSN 2615-9678

+ Electric field: 0.5, 0.6, 0.7, and 0.8 kV·cm^{-1}.

+ Spray rate: 0.3, 0.4, 0.5, and 0.6 mL·h^{-1}.

We found the optimal conditions as follows: TTip/PVP volume ratio 2:1, spray rate 0.4 mL·h^{-1}, and electric field 0.6 kV·cm^{-1}.

To investigate the photoelectrochemical properties of the material, we sprayed the TTip/PVP fibres on the ITO substrate for 20 min. After spraying, the electrodes were calcined at 500 °C in the air for 2 h with a heating rate of 2 °C·min^{-1}. We obtained TiO_2/ITO nanostructured fibre electrodes.

2.3 Characterization

The morphological structure of the fabricated material was examined with field-emission scanning electron microscopy (FE-SEM, Hitachi S4800), and transmission electron microscopy (TEM, JEOL JEM-2100F). The distribution of samples was measured with FE-SEM equipped with an energy-dispersive X-ray spectrometer (EDX). The structures and optical properties of samples were analyzed with X-ray diffraction (XRD, Bruker D2) with Cu Kα radiation and a UV-vis spectrophotometer (Jasco V-770).

2.4 Photoelectrochemical measurement

The PEC properties were investigated by using a three-electrode electrochemical analyzer (Potentiostat/Galvanostat model CS350) with the fabricated nanostructure films formed on an ITO substrate as a working electrode, a platinum (Pt) wire as a counter electrode, and Ag/AgCl in saturated KCl as a reference electrode. The electrolyte is a 0.5 M Na_2SO_4 solution. The simulated sunlight source is a 150 W Xe lamp (Gloria-X150A) with an intensity of 100 mW·cm^{-2}. All the measurements were performed with front-side illumination of the photoanodes. The potential was swept linearly at a scan rate of 10 mV·s^{-1} with the potential range from –0.6 to 0.6 V (vs Ag/AgCl). The electrode illuminated area exposed to the electrolyte was fixed at 1 cm^2 by using nonconductive epoxy resin. The conversion efficiency was calculated following the equation

$$\eta\ (\%) = J_P \times (E_{rev} - E_{app}) \times 100/I_0 \quad (1)$$

where J_P is the photocurrent density (mA·cm^{-2}); I_0 is the irradiance intensity of the incident light (100 mW·cm^{-2}); E_{rev} is the standard state-reversible potential (1.23V vs NHE); E_{app} (= $E_{meas} - E_{aoc}$) is the applied potential, where E_{meas} is the electrode potential of the working electrode at which the photocurrent was measured under illumination; E_{aoc} is the electrode potential of the same working electrode under open circuit conditions.

3 Results and discussion

3.1 Effect of TTip/PVP mass ratios

Fig. 1 presents the SEM images of the samples manufactured at different TTip/PVP mass ratios. The images show that the 3:1 ratio (Fig. 1a) does not form fibres. The fibres are stuck together because of the small polymer portion in the spray solution. At the 2.5:1 ratio (Fig. 1b), titanium salt begins to form several short fibres. The fibres form more clearly at the ratio 2:1 (Fig. 1c) and 1.5:1 (Fig. 1d). However, at the ratio of 1.5:1, the fibres are uneven because of the liquid's high viscosity that hinders the spraying process. We also reduced the ratio to 1:1, but the viscosity

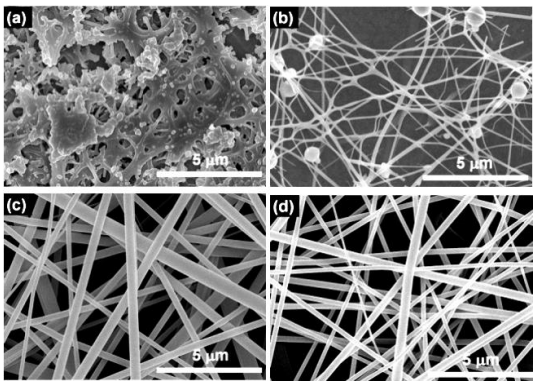

Fig. 1. SEM images of Ti^{2+}/PVP material prepared under conditions: electric field 0.6 kV·cm^{-1}, spray rate 0.01 mL·h^{-1}, and TTip/PVP mass ratios: (a) 3:1, (b) 2.5:1, (c) 2:1, (d) 1.5:1

became so high that the solution froze at the syringe tip.

These results indicate that the TTip/PVP mass ratios between 1.8:1 and 2.2:1 are suitable for the electrospinning process. Of course, PVP molecular mass also affects the formation of the fibres. Therefore, we choose a TTip/PVP ratio of 2:1 for the subsequent experiments.

3.2 Effect of electric fields

Fig. 2 shows the SEM images of Ti^{2+}/PVP material fabricated at different electric fields. The continuous fibres with several hundred-micrometre lengths were formed at all electric field values with a relatively smooth surface. They distribute randomly in all directions, overlapping and creating a thin film on the substrate. From the SEM images, we calculated the average fibre diameter (Table 1) and displayed the diameter distribution (Fig. 3).

It can be seen that the diameter of Ti^{2+}/PVP fibre decreases as the electric field increases. This decreasing trend is consistent with that of previous research [10, 11]. We found that at the 0.4 kV·cm^{-1} electric field, the fibre does not form. Thus, the electric field of 0.5 kV·cm^{-1} is neccessary to create inductive charges in the spray solution and causes the electrostatic force to form fibres.

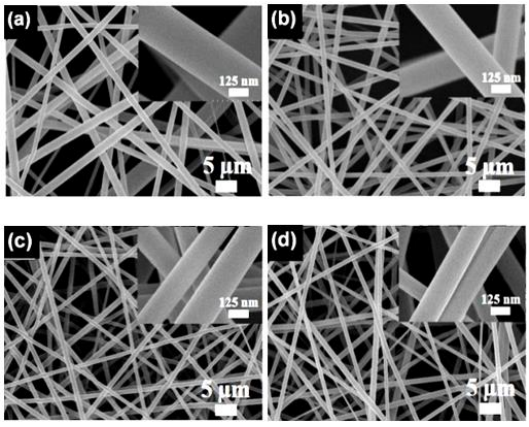

Fig. 2. SEM image of Ti^{2+}/PVP material prepared under conditions: TTip/PVP mass ratio 2:1, spray rate 0.01 mL·h^{-1}, electric spray fields: (a) 0.5 kV·cm^{-1}; (b) 0.6 kV·cm^{-1}; (c) 0.7 kV·cm^{-1}; (d) 0.8 kV·cm^{-1}

Table 1. Average fibre diameter at different electric fields

Electric field (kV·cm^{-1})	Average fibre diameter (nm)
0.5	400 ± 90
0.6	273 ± 18
0.7	246 ± 24
0.8	220 ± 23

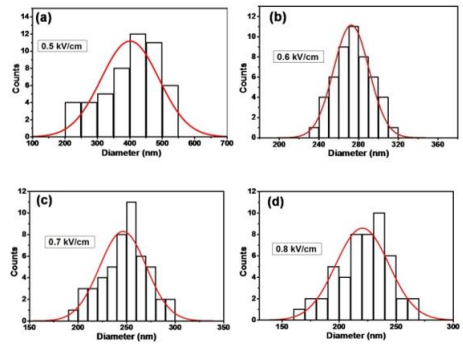

Fig. 3. Fibre diameter distribution at electric fields: (a) 0.5 kV·cm^{-1}, (b) 0.6 kV·cm^{-1}, (c) 0.7 kV·cm^{-1}, (d) 0.8 kV·cm^{-1}

The table shows that the fibre diameter decreases significantly as the electric field increases from 0.5 to 0.6 kV·cm^{-1}, with a slower decline up to 0.8 kV·cm^{-1}. Maybe, at the electric field of 0.6 kV·cm^{-1}, the inductive charges do not change much, causing the fibre diameter to decrease slightly when the electric field increases to 0.8 kV·cm^{-1}.

Although the fibre diameter is relatively large (273 nm) at the electric field of 0.6 kV·cm^{-1}, it is highly uniform (relative error 6.6%), and spinning does not break. Low et al. [11] reported that it was possible to fabricate fibres with an average diameter of 70 nm at an electric field of 2.2 kV·cm^{-1}, but the diameters were uneven (about 50% relative error). Therefore, we choose the electric field of 0.6 kV·cm^{-1} for the fabrication of photoelectrodes.

3.3 Effect of spray rates

The SEM images of Ti^{2+}/PVP materials at different spray rates are shown in Fig. 4. At the spray rate

pISSN 1859-1388
eISSN 2615-9678

of 0.3 mL·h^{-1} (Fig. 4a) and 0.4 mL·h^{-1} (Fig. 4b), the fibre diameter is relatively uniform, and the spray is continuous. When the spray rate increases to 0.5 and 0.6 mL·h^{-1}, the fibre diameter becomes smaller and uneven. The higher the spray rate, the more uniformity of the fibre diameter decreases, and the spraying process is interrupted. This result indicates that, at the spray rates of 0.3–0.4 mL·h^{-1}, the amount of solution supplied for the spinning process is sufficient, so the fibre diameter is uniform with continuous spinning.

We calculated the diameter distribution of the fibres at the spray rate of 0.3 and 0.4 mL·h^{-1} from SEM images, thereby determining the average diameter of the fibre. The results are shown in Fig. 5.

The figure shows that the fibre diameter does not differ much between the two spray rates. At the 0.4 mL·h^{-1} rate, the fibre diameter changes less (relative error of 5.8% compared with 19.1 % at the spray rate of 0.3 mL·h^{-1}). Thus, the spray rate of 0.4 mL·h^{-1} is consistent with the electric field we chose above.

After all, the optimal conditions for fabricating the nanofibre Ti^{2+}/PVP material are as follows: mass concentration of the PVP solution, 8%; TTiP/PVP mass ratio, 2:1; electric field, 0.6 kV·cm^{-1}; spray rate, 0.4 mL·h^{-1}.

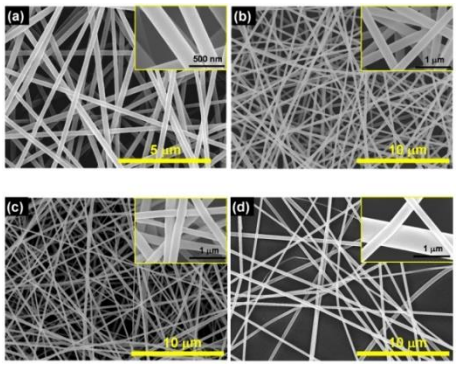

Fig. 4. SEM images of Ti^{2+}/PVP material prepared under conditions: TTip/PVP mass ratio 2:1, electric field of 0.6 kV·cm^{-1}, and spray rates: (a) 0.3 mL·h^{-1}, (b) 0.4 mL·h^{-1}, (c) 0.5 mL·h^{-1}, and (d) 0.6 mL·h^{-1}

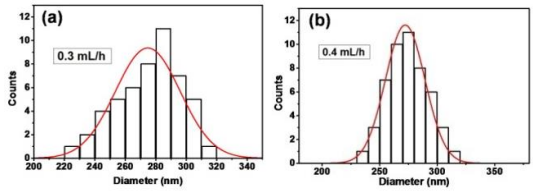

Fig. 5. Fibre diameter distribution at spray rates: (a) 0.3 mL·h^{-1} and (b) 0.4 mL·h^{-1}

The X-ray diffractogram of the Ti^{2+}/PVP indicates that the material exists in the amorphous form (Fig. 6, lower line). Thus, the TTip salt, after hydrolysis to Ti(OH)$_4$ in the PVP lattice, has an amorphous structure. After calcining, it becomes crystalline with characteristic diffraction at 2θ of 25.26, 37.78, 48.00, and 53.90° (Fig. 6, upper line). These peaks correspond to the lattice planes (101), (004), (200), (211), and (213) of the anatase TiO$_2$, with no peak positions corresponding to the other substances (according to JCPDS standard card number 84-1286). This information proves that the PVP polymer is completely burned during calcining. The diameter of the TiO$_2$ fibres is 15 nm, calculated according to the Scherrer formula. These results are consistent with some previously published results [9, 11]. According to Kim, when the heating temperature increases to 600 °C, there is a transition from the anatase to rutile phases [12]. Because the ITO substrate used in the experiment breaks at 550 °C, we did not investigate the phase transition of TiO$_2$ fibres according to the calcining temperature.

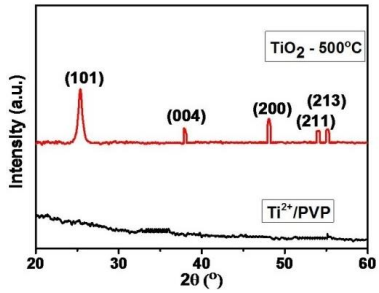

Fig. 6. X-ray diffractograms of Ti^{2+}/PVP fibre and TiO$_2$ fibre calcined at 500 °C for 2 h

Fig. 7a shows the SEM image of the material after calcining at 500 °C for two hours.

The material retains the same fibre shape, with a smaller diameter and lower fibre density. There are breaks in some fibres, and the fibre surface is rougher after calcining. The reason is that the PVP is completely burned when calcined at 500 °C, causing the fibre diameter to decrease. At the same time, polymer burning creates space between the TiO_2 fibres, which is favourable for surface modification of fibres with other semiconductors.

Based on the fibre diameter distribution diagram (Fig. 7c), we found the average diameter of the TiO_2 fibre to be 132 ± 16 nm. The EDS diagram also shows that the material after calcining consists of elements titanium and oxygen (the presence of C is due to carbon mesh when measuring SEM, and Si is due to the glass substrate coated with TiO_2 fibres).

The TEM image shows that TiO_2 fibres are formed from TiO_2 particles bonding together because the PVP is lost upon calcining. The TiO_2 particle has a size of 12 nm (Fig. 8a). The lattice planes were determined from the HR-TEM image (Fig. 8b). The lattice planes corresponding to the TiO_2 anatase crystal are (101) (d_{101} = 0.35 nm) and (004) (d_{004} = 0.24 nm). This result is completely consistent with those of the X-ray diffraction above.

Fig. 9 shows the optical current density and optical conversion efficiency of nanofibre structure TiO_2 electrodes at 20 min spraying. Under the irradiation of the Xenon lamp, the optical current increases as the external potential increases and reaches the saturation value at 0.55 V. The photoelectric conversion efficiency is 0.027% (at a voltage of 0.2 V and a current density of 80 $\mu A \cdot cm^{-2}$) (Fig. 9b). The film thickness corresponding to 20-min spraying is 3 μm (Fig. 9c). The highest optical current density of the sample in this study is roughly equivalent to that of some published TiO_2 structures [9, 13].

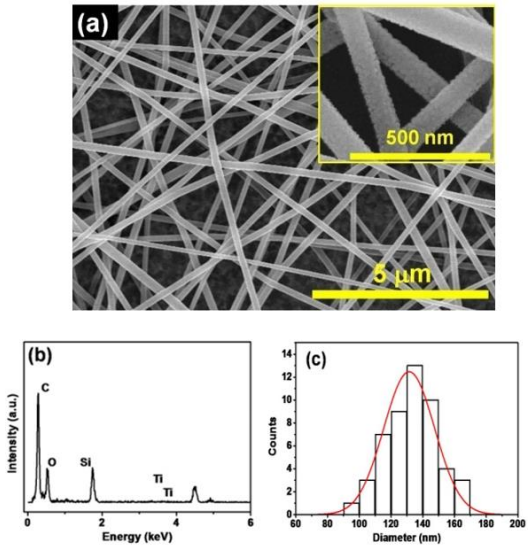

Fig. 7. SEM image (a), EDS spectral diagram (b), and diameter distribution diagram of TiO_2 fibre calcined at 500 °C (c)

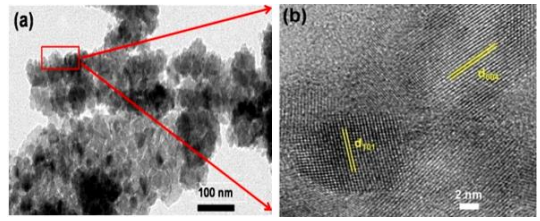

Fig. 8. TEM (a) and HR-TEM (b) images of TiO_2 fibre calcined at 500 °C

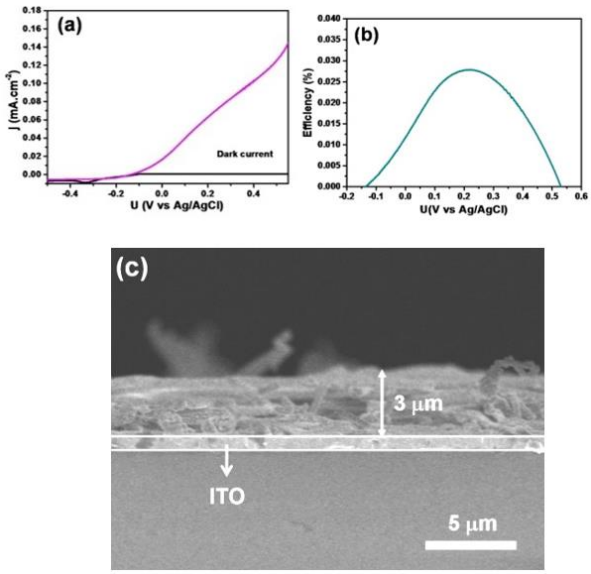

Fig. 9. Optical current density (a), photoelectric conversion efficiency (b), and film thickness corresponding to the 20 min spray time (c)

pISSN 1859-1388
eISSN 2615-9678

The photoelectrochemical properties indicate that the TiO_2 nanofibre structures are very promising for applications in photoelectrochemistry.

4 Conclusion

Our study shows that TiO_2 nanofibre structure was successfully synthesized with the electrospinning method. This structure is favourable for later surface modification with other semiconductors. The TiO_2 nanofibre-based photoanode exhibits excellent photocurrent density, equivalent to the optical current density of some TiO_2 structures reported so far. The photoanode is potential for energy storage and conversion applications.

References

1. Fujishima A, Honda K. Electrochemical Photolysis of Water at a Semiconductor Electrode. Nature. 1972;238(5358):37-8.
2. Khan SUM, Al-Shahry M, Ingler WB. Efficient photochemical water splitting by a chemically modified n-TiO_2.Science. 2002;297(5590):2243-5.
3. Hu L, Chen G. Analysis of Optical Absorption in Silicon Nanowire Arrays for Photovoltaic Applications. Nano Letters. 2007;7(11):3249-52.
4. Mor GK, Shankar K, Paulose M, Varghese OK, Grimes CA. Enhanced Photocleavage of Water Using Titania Nanotube Arrays. Nano Letters. 2005;5(1):191-5.
5. Kang Q, Cao J, Zhang Y, Liu L, Xu H, Ye J. Reduced TiO_2 nanotube arrays for photoelectrochemical water splitting. Journal of Materials Chemistry A. 2013;1(18):5766-74.
6. Feng X, Shankar K, Varghese OK, Paulose M, Latempa TJ, Grimes CA. Vertically Aligned Single Crystal TiO_2 Nanowire Arrays Grown Directly on Transparent Conducting Oxide Coated Glass: Synthesis Details and Applications. Nano Letters. 2008;8(11):3781-6.
7. Qin D-D, Bi Y-P, Feng X-J, Wang W, Barber GD, Wang T, et al. Hydrothermal Growth and Photoelectrochemistry of Highly Oriented, Crystalline Anatase TiO_2 Nanorods on Transparent Conducting Electrodes. Chemistry of Materials. 2015;27(12):4180-3.
8. Mali MG, An S, Liou M, Al-Deyab SS, Yoon SS. Photoelectrochemical solar water splitting using electrospun TiO_2 nanofibers. Applied Surface Science. 2015;328:109-14.
9. Li Y, Gao F, Zhao L, Ye Y, Liu J, Tao Y. Reversing CdS and ZnS preparation order on electrospun TiO_2 and its effects on photoelectrochemical property. 2016;11(11):731-3.
10. Kumar A, Jose R, Fujihara K, Wang J, Ramakrishna S. Structural and Optical Properties of Electrospun TiO_2 Nanofibers. Chemistry of Materials. 2007;19(26):6536-42.
11. Albetran H, Dong Y, Low IM. Characterization and optimization of electrospun TiO_2/PVP nanofibers using Taguchi design of experiment method. Journal of Asian Ceramic Societies. 2015;3(3):292-300.
12. Kim J-H, Lee J-H, Kim J-Y, Kim SS. Synthesis of Aligned TiO_2 Nanofibers Using Electrospinning. 2018;8(2):309.
13. Li L, Dai H, Feng L, Luo D, Wang S, Sun X. Enhance photoelectrochemical hydrogen-generation activity and stability of TiO_2 nanorod arrays sensitized by PbS and CdS quantum dots under UV-visible light. Nanoscale Research Letters. 2015;10(1):418.